Dynamics of Spatial Degrees-of-Freedom in MIMO Mobile Channels

Katsuyuki Haneda, Afroza Khatun, Veli-Matti Kolmonen, and Jussi Salmi

Aalto University School of Electrical Engineering, SMARAD Centre of Excellence, Finland
#katsuyuki.haneda@aalto.fi

***Abstract*—This paper presents insights on spatial degrees-of-freedom (SDoF) of multiple-input multiple-output (MIMO) mobile propagation channels. The SDoF depends on multipath richness of the propagation channel and antenna aperture size, and indicates the number of effective antenna elements for the spatial multiplexing on the antenna aperture. We first define the SDoF using expression of propagation channels in plane and spherical wave domains. The SDoF is estimated for indoor MIMO mobile scenarios based on measurements, revealing that at least two SDoFs corresponding to two orthogonal polarizations are always available. Furthermore, the SDoF is mostly less than 10 when the antenna aperture size at the base and mobile sides is $3\lambda^2$, and less than 4 if the aperture size is $0.25\lambda^2$, revealing feasibility of spatial multiplexing with at most 4 eigenmodes using an electrically small antenna aperture at the mobile end. Significant fluctuation of the SDoF is observed during a mobile is in motion even though there is always a line-of-sight (LOS). The fluctuation is attributed to difference in LOS path dominance over other multipath components and varying angular distribution of the multipaths.**

I. Introduction

It is well-known that multiple-input multiple-output (MIMO) radio communications benefit from multipath propagation [1] and from proper design of antenna arrays at communication devices [2] to improve the channel capacity. Among different radio transmission techniques that utilize the spatial domain, the spatial multiplexing is most promising for increasing the channel capacity by exploiting eigenmodes of radio channels for parallel data streaming. The potential of the spatial multiplexing in radio channels has been quantified and discussed by several metrics, such as the channel capacity, the number of dominant eigenmodes, and the eigenvalue dispersion [3]. When these metrics are evaluated with a specific configuration of antenna arrays, applicability of the results is limited to the evaluated antenna configuration only. In order to obtain more generic estimates of the metrics for various antenna types, we evaluate the number of dominant eigenmodes, so called a spatial degrees-of-freedom (SDoF), which depend on the radio propagation condition and the antenna aperture size, but are otherwise independent of the antenna elements and geometry. The SDoF indicates the effective number of antenna elements on the aperture that can contribute to the increase of the channel capacity through spatial multiplexing. Estimation methods of the SDoF for multiple antenna channels are studied by Poon *et al.* [4], [5]. Estimation of the SDoF in measured radio channels are discussed in [6], [7] for different propagation conditions such as line-of-sight (LOS) and non-LOS scenarios. However, the reports concern too idealistic or a limited number of measured radio channels, and do not address dynamics of the SDoF in mobile propagation scenarios. The dynamic behavior of the SDoF in mobile scenarios is an important factor for multi-element antenna design where the goal is to obtain a generally working structure for various different radio propagation conditions during a mobile is in motion.

This paper describes methodologies to estimate the SDoF from measured MIMO radio channels in an indoor mobile environment at 5.3 GHz radio frequency. To this end, we first discuss the de-embedding of antenna element characteristics from the measured radio channels in the plane and spherical wave domains. We then define the SDoF based on the response of the propagation channel, which depends only on the transmit (Tx) and receive (Rx) antenna aperture size. In our analysis, effects of antenna superdirectivity [8] is ruled out. The results revealed that at least two SDoFs corresponding to two orthogonal polarizations are always available. Furthermore, the SDoF is mostly less than 10 when the antenna aperture size at the Tx and Rx is $3\lambda^2$, and less than 4 if the aperture size is $0.25\lambda^2$. The SDoF fluctuates during the mobile motion due to rapid change of local scattering environments even under a LOS channel condition.

II. Spatial Degrees-of-Freedom

For the purpose of deriving the SDoF that does not depend on antenna element realizations on the aperture, we first make a distinction between the radio channel, which includes all effects of the antennas and the propagation channel, and the propagation channel itself, which is only influenced by the aperture size of the Tx and Rx antennas. Then the SDoF is defined based on the expression of the propagation channel.

A. The Propagation Channel

A narrowband propagation channel observed with a certain Tx and Rx antenna is usually described by a set of plane waves as [9]

$$\mathcal{P}_{\rm p} = \{\boldsymbol{\alpha}_l, \boldsymbol{\Gamma}_l, \boldsymbol{\Gamma}'_l\}_{l=1}^{L}, \quad (1)$$

where $\boldsymbol{\alpha} \in \mathbb{C}^{2\times 2}$ is a polarimetric complex amplitude, $\boldsymbol{\Gamma} = [\phi\ \theta]$ and $\boldsymbol{\Gamma}' = [\phi'\ \theta']$ are vectors composed of the azimuth and polar angles on the Tx and Rx sides, respectively, and subscript a_l means for the l-th plane wave.

978-88-907018-1-8/13/$31.00 ©2013 IEEE

The plane wave expression of the propagation channel corresponds to the one in the spherical wave domain as [10]

$$\mathcal{P}_{\mathrm{s}} = \{R_{j'j}\}_{j=1,j'=1}^{\infty}, \tag{2}$$

where

$$R_{j'j} = \sum_{l=1}^{L} \boldsymbol{f}_{j'}^{H}(\boldsymbol{\Gamma}_l)\boldsymbol{\alpha}_l \boldsymbol{f}_j(\boldsymbol{\Gamma}'_l), \tag{3}$$

$\boldsymbol{f}_j(\boldsymbol{\Gamma}) = [f_{\mathrm{V},smn}(\boldsymbol{\Gamma})\ f_{\mathrm{H},smn}(\boldsymbol{\Gamma})]^T$ are the far-field electric field of the j-th spherical wavemode for the directions of the l-th plane wave and $\cdot^T$ and $\cdot^H$ denote the transpose and Hermitian-transpose operations. The index j is related to the s, m, and n-th modes of the spherical waves as $j = 2\{n(n+1)+m-1\}+s$ [11]. We stress that $\boldsymbol{f}$ is *not* an antenna radiation pattern, but is the basis function, *i.e.*, the operator of the spherical Fourier transform to convert from plane to spherical wave domains defined as

$$f_{\mathrm{V},1mn}(\boldsymbol{\Gamma}) = k_{mn}(-\mathrm{j})^{n+1}\left(\frac{\mathrm{j}m\bar{P}_n^{|m|}(\cos\theta)}{\sin\theta}\right), \tag{4}$$

$$f_{\mathrm{H},1mn}(\boldsymbol{\Gamma}) = k_{mn}(-\mathrm{j})^{n+1}\left(-\frac{\mathrm{d}}{\mathrm{d}\theta}\bar{P}_n^{|m|}(\cos\theta)\right), \tag{5}$$

$$f_{\mathrm{V},2mn}(\boldsymbol{\Gamma}) = k_{mn}(-\mathrm{j})^{n}\left(\frac{\mathrm{d}}{\mathrm{d}\theta}\bar{P}_n^{|m|}(\cos\theta)\right), \tag{6}$$

$$f_{\mathrm{H},2mn}(\boldsymbol{\Gamma}) = k_{mn}(-\mathrm{j})^{n}\left(\frac{\mathrm{j}m\bar{P}_n^{|m|}(\cos\theta)}{\sin\theta}\right), \tag{7}$$

$$k_{mn} = \frac{2}{\sqrt{2n(n+1)}}\left(-\frac{m}{|m|}\right)^m e^{\mathrm{j}m\phi}, \tag{8}$$

where $\bar{P}_n^{|m|}(\cdot)$ is the normalized associated Legendre function with the order of m.

The spherical waves can express the propagation channel by a matrix $\boldsymbol{R}$ having a coefficient $R_{j'j}$ as an entry to the j-th row and j'-th column, while the plane wave expression needs to have both the angles and the complex amplitude of the multipath components to describe the propagation channel.

B. The Radio Channel

A narrowband radio channel includes effects of antennas and propagation channel. It is expressed by the sum of L plane waves weighted by the Tx and Rx antenna patterns as

$$h = \sum_{l=1}^{L} \boldsymbol{a}'^{H}(\boldsymbol{\Gamma}'_l)\boldsymbol{\alpha}_l \boldsymbol{a}(\boldsymbol{\Gamma}_l) \tag{9}$$

where $\boldsymbol{a}(\boldsymbol{\Gamma}) = \boldsymbol{g}(\boldsymbol{\Gamma})\exp\{\mathrm{j}k_0\langle\boldsymbol{u},\boldsymbol{d}\rangle\}$, the operation $\langle\boldsymbol{a},\boldsymbol{b}\rangle$ denotes an inner product of the vectors $\boldsymbol{a}$ and $\boldsymbol{b}$, $\boldsymbol{g}(\boldsymbol{\Gamma}) = [g_{\mathrm{V}}(\boldsymbol{\Gamma})\ g_{\mathrm{H}}(\boldsymbol{\Gamma})]^T$ is a far-field radiation pattern of the antenna element in the direction $\boldsymbol{\Gamma}$, $\boldsymbol{d}$ is the position vector of the antenna element, and finally,

$$\boldsymbol{u} = [\sin\theta\cos\phi \quad \sin\theta\sin\phi \quad \cos\theta]^T. \tag{10}$$

The narrowband radio channel can also be expressed by the spherical wave coefficients of the propagation channel $\boldsymbol{R}$ as [12]

$$h = \boldsymbol{q}'^{H}\boldsymbol{R}\boldsymbol{q} \tag{11}$$

where $\boldsymbol{q}$ and $\boldsymbol{q}'$ are the spherical wave coefficient vectors for the Tx and Rx antennas. They are related to the far-field radiation pattern as

$$\boldsymbol{a}(\boldsymbol{\Gamma}) = \sum_{j=1}^{\infty} \boldsymbol{f}_j(\boldsymbol{\Gamma})q_j \tag{12}$$

for all the possible directions $\boldsymbol{\Gamma}$. The radio channels given by (9) and (11) constitute a single entry of the channel matrix in a MIMO system.

C. Spatial Degrees-of-Freedom

The SDoF of the radio channel is determined by the inherent multipath richness of the propagation channel and the Tx and Rx antenna aperture size [4]. For a given multipath richness, a larger value of the SDoF can be observed when using larger antenna aperture at the Tx *and* Rx. Concretely, based on the plane wave expression of the radio channel (9), the larger antennas can produce narrower beams in the angular domain and thus allow more non-overlapping pathways to illuminate the physical scatterers in the channel.

The SDoF can also be explained by the spherical wave expressions in (11). The number of dominant spherical wavemodes is determined by the Tx and Rx antenna aperture size because of the mode truncation property [11]. A rule of thumb of the truncation is expressed in terms of the n-modes representing the polar angle characteristics as

$$N = \lfloor k_0 r_0 \rfloor + \epsilon, \tag{13}$$

where k_0 is a wavenumber in the free space, r_0 is a minimum radius enclosing the whole volume of the antenna, $\lfloor\cdot\rfloor$ is the floor function, and ϵ is an uncertainty factor taking values between 0 and 10 for practical antennas [11]. The truncation n-mode, N, is related to the total number of dominant spherical wavemodes as $J = 2N(N+2)$. Therefore larger antenna aperture can support more spherical wavemodes to propagate over the channel, leading to larger SDoF. The SDoF of the propagation channel D is given by the rank of $\boldsymbol{R} \in \mathbb{C}^{J'\times J}$. A rank of any MIMO channels realized by antenna elements on the aperture is upper-bounded by D [6].

III. MIMO Mobile Channel Sounding and Modeling

A. MIMO Channel Sounding

In order to investigate the SDoF in MIMO mobile channels, a set of channel sounding data from an indoor hall scenario are used. Floor plan of the measurement site is shown in Fig. 1. Both the BS and mobile were on the second floor of the hall and were elevated by 2 m above the floor. The mobile antenna was mounted on a trolley and moving with slower speed than a pedestrian, *i.e.*, 1 m/s. The BS was located at the center of the hall on a balcony bridging two sides of the hall. The mobile route "A" ran along a balcony on the longitudinal side of the hall having LOS to the BS almost all the time. The route "B" was on another balcony running perpendicular to the route "A" where the mobile came closest to the BS around

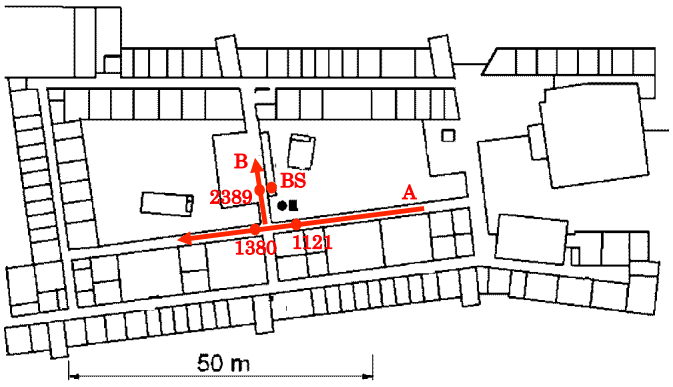

Fig. 1. Physical environment of the MIMO channel sounding in an indoor scenario. Indices of three mobile locations that will be discussed in later sections are marked on the routes.

location 2389 as indicated in Fig. 1. The length of the two routes amounts to 40 and 15 m, respectively.

A wideband channel sounder operating at 5.3 GHz with 60 MHz bandwidth was used to collect MIMO channel responses. Semi-spherical antenna arrays were used at the BS and mobile ends. Radiation patterns of the antenna arrays cover almost an entire solid angle except for $\pm z$ directions. The arrays consist of 16 dual-polarized patch antenna elements leading to 32 feeds, and their aperture size is about $3\lambda^2$ at 5.3 GHz. The number of antenna elements are much larger than the estimated SDoF as we describe in Section IV. MIMO channel responses were measured at every 39 ms during the mobile is running. Details of the wideband MIMO channel sounders and antenna arrays are found in [13].

B. MIMO Channel Modeling

Parameters of the multipath plane waves were estimated from the measured wideband MIMO channel responses using a high resolution algorithm [14]. The estimated parameters include the ones in (1), namely the azimuth and polar angles at the Tx and Rx and complex polarimetric amplitude of each multipath. Since we assume downlink communications from the BS to mobile, they can be referred to as the Tx and Rx interchangeably in the following discussions. Propagation delays are also estimated, but are not used in the present SDoF analysis assuming flat-fading characteristics of the channel. The parameter estimation involves radiation patterns of the Tx and Rx antennas to calibrate their effects on the estimated parameters. Therefore the parameters represent characteristics of the propagation channel seen from the Tx and Rx antenna aperture. There were more than 50 multipaths at each mobile location, and they were attributed to a LOS, specular reflections from walls and floor, and diffraction and scattering from corners of stairs. The multipath consisted of at least 50 % of the total power of the channel and the rest was classified into distributed diffuse scattering [15].

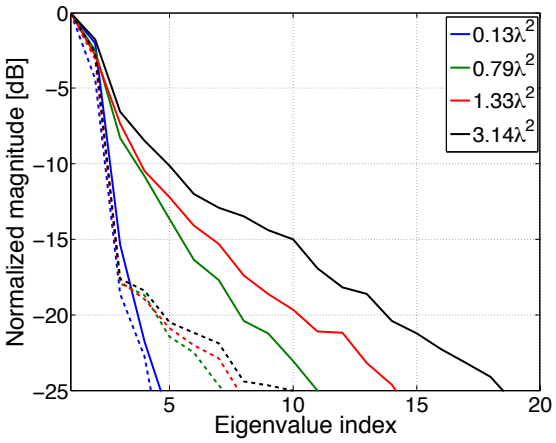

(a)

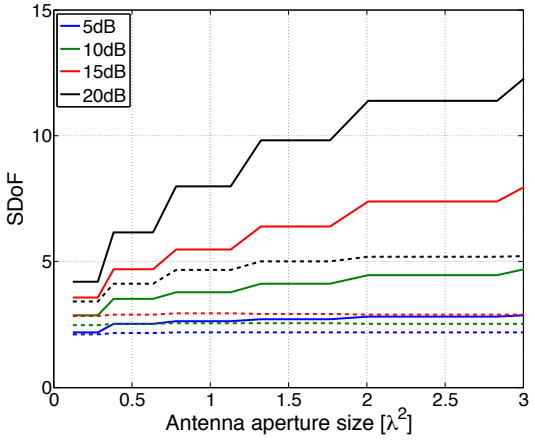

(b)

Fig. 2. (a) Eigenvalue distributions of $\boldsymbol{R}$ for different antenna aperture size. (b) SDoF variation over different antenna aperture size. There are 4 curves in each figure representing the SDoF defined by $t = 5$, 10, 15, and 20 dB threshold levels in determining the number of dominant eigenvalues. The solid and dashed lines correspond to the results from mobile locations 1380 and 1121 defined in Fig. 1, respectively.

IV. Results and Discussions

A. SDoF Estimation

The SDoF is given by the rank of the propagation channel $\boldsymbol{R}$. To this end, the plane wave parameter estimates are converted to the spherical wave expression using (3). The dimension of $\boldsymbol{R}$ was determined by the antenna aperture size in (13) with $\epsilon = 0$. The Tx and Rx antenna aperture size is considered identical in this analysis, hence $\boldsymbol{R}$ is always a square matrix. Figure 2(a) shows an eigenvalue distribution of $\boldsymbol{R}$ at two mobile locations on route "A". The eigenvalue distributions are shown for various antenna aperture sizes. Larger antenna aperture gives rise to more eigenvalues visible in the figure because of the increased capability of the antenna aperture to resolve multipaths in the angular domain. We define the rank estimates to be the number of eigenvalues exceeding $-t$ dB in magnitude relative to the strongest one, where $t = 5, 10, 15$, and 20 are tested in our analysis. In

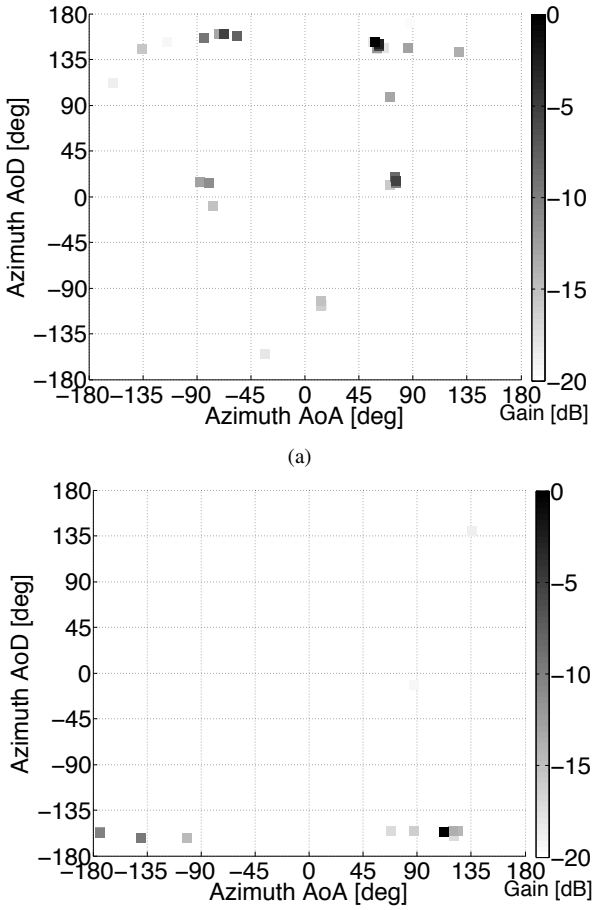

(a)

(b)

Fig. 3. Distribution of plane wave propagation paths on the azimuth AoA–AoD domain at mobile locations (a) 1380 and (b) 1121. They result in the solid and dashed lines in Figs. 2.

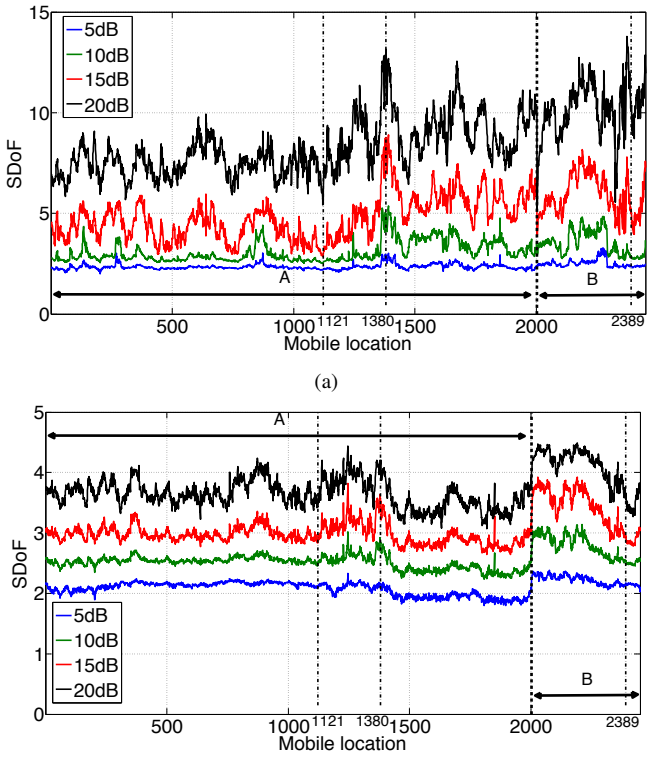

(a)

(b)

Fig. 4. SDoF of the MIMO propagation channels at identical antenna aperture sizes of the BS and mobile with (a) $3\lambda^2$ and (b) $0.25\lambda^2$. There are 4 curves in each figure representing the SDoF defined by $t = 5$, 10, 15, and 20 dB threshold levels in determining the number of dominant eigenvalues.

deriving the SDoF, the effect of the small-scale fading is averaged out by taking the mean over the rank estimates from 100 realizations of $\boldsymbol{R}$. Different realizations of $\boldsymbol{R}$ were obtained by adding a random phase to the complex amplitude of the propagation paths $\boldsymbol{\alpha}$ [16]. Figure 2(b) shows variation of the SDoF on antenna aperture size for different threshold levels. Though the two mobile locations have an LOS to the BS, the SDoF shows significantly different characteristics. The SDoF does not increase even if antenna aperture size is larger in the mobile location 1121 except for the threshold level $t = 20$. For antenna aperture size of $3\lambda^2$ with $t = 20$, the SDoF for mobile location 1380 revealed more than twice of that at location 1121. The difference can be explained by a local scattering environment of propagation channels. Figures 3 illustrate distribution of propagation paths on the azimuth angle-of-departure (AoD) and angle-of-arrival (AoA) domain at the BS and mobile, respectively. Within 20 dB power range relative to the strongest path, the path distribution at location 1380 shows more multipaths and wider angular range over the AoA-AoD domain than at location 1121. The propagation paths depart almost to a single direction at the BS for location 1121 and restrict overall multipath richness of the MIMO channel. The SDoF is determined by the lower of that on the Tx and Rx sides [4].

B. *Variation of the SDoF in Different Environments*

Figure 4 shows the estimated SDoF for the considered mobile routes at identical Tx and Rx antenna aperture sizes of $3\lambda^2$ and $0.25\lambda^2$. The SDoF with $t = 5$ dB stays around two in most mobile locations because the strongest multipaths support two orthogonal polarizations. As the threshold level t and the antenna aperture size increase, fluctuation of the SDoF is more significant. At $3\lambda^2$ antenna aperture size, the largest SDoF can be as twice high as the smallest value due to drastic variation of the local scattering environment even if an LOS always exists. The same observation can be obtained from route "B" where the distance between the BS and mobile is the shortest at location 2389. According to Fig. 4, the SDoF does not reveal any special characteristics at the location. As exemplified in Figs. 3, a small SDoF appears when LOS has much stronger power than other multipaths, while being able to see more multipaths leads to a larger SDoF. Also distribution of the propagation paths on the angular domain determines the SDoF. There is less fluctuation in SDoF with $0.25\lambda^2$ antenna aperture size because of less capability of the antenna aperture to resolve multipaths in the angular domain. Still, the SDoF

shows up to 4 if the threshold is 15 or 20 dB, indicating feasibility of spatial multiplexing with at most 4 eigenmodes using an electrically small antenna aperture. Since the antenna aperture size is asymmetric at the BS and mobile ends in mobile communications, overall SDoF of single-user MIMO mobile channels is restricted by the smaller antenna aperture size of the two sides, *i.e.*, at the mobile end.

V. Conclusions

This paper provided insights on the SDoF in MIMO mobile propagation channels. We showed that the SDoF depends on multipath richness of propagation channels and antenna aperture size, and is independent of realization of antenna elements on the aperture. Having described the methodology to estimate the SDoF from measured propagation channels, we showed that there are at least two SDoFs for 5 dB threshold level relative to the strongest eigenmode because of the availability of two orthogonal polarizations in propagation channels. The SDoF with 20 dB threshold level is mostly in the range of 5 to 10 and 3 to 4 for the identical BS and mobile antenna aperture sizes of $3\lambda^2$ and $0.25\lambda^2$, respectively. The result reveals the feasibility of spatial multiplexing with at most 4 eigenmodes using an electrically small mobile antenna. When the antenna aperture size and the threshold value is large, the SDoF is subject to large variation due to different local scattering around the BS and mobile even in the presence of an LOS. The SDoF gives us an insight on the effective number of antenna elements that works on the aperture for spatial multiplexing. The threshold level t serves as a reference to a receiving signal-to-noise ratio in which a mobile operates. That is, if the receiving signal-to-noise ratio is 20 dB on average, it is sufficient to implement at most 10 and 4 antenna elements on $3\lambda^2$ and $0.25\lambda^2$ aperture, respectively.

Acknowledgment

The authors would like to thank the SMARAD Centre of Excellence by the Academy of Finland for their financial support.

References

[1] E. Telatar, "Capacity of multi-antenna Gaussian channels," *Euro. Trans. Telecommun.*, vol. 10, no. 6, pp. 585–596, Nov. 1999.

[2] T. S. Pollock, T. D. Abhayapala, and R. A. Kennedy, "Antenna saturation effects on MIMO capacity," *Proc. IEEE Int. Conf. Commun.*, vol. 3, pp. 2301–2305, Anchorage, AK, May 2003.

[3] J. Salo, P. Suvikunnas, H. M. El-Sallabi, and P. Vainikainen, "Ellipticity statistic as measure of MIMO multipath richness," *Elec. Lett.*, vol. 42, no. 3, pp. 160–162, Feb. 2006.

[4] A. S. Y. Poon, R. W. Brodersen, and D. N. C. Tse, "Degrees of fredom in multiple-antenna channels: a signal space approach," *IEEE Trans. Inf. Theory,* vol. 51, no. 2, pp. 523–536, Feb. 2005.

[5] A. S. Y. Poon, D. N. C. Tse, and R. W. Broadersen, "Impact of scattering on the capacity, diversity, and propagation range of multiple-antenna channels," *IEEE Trans. Inf. Theory*, vol. 52, no. 3, pp. 1087–1100, Mar. 2006.

[6] K. Haneda, A. Khatun, M. Dashti, T. Laitinen, V.-M. Kolmonen, J. Takada, and P. Vainikainen, "Measurement-based evaluation of the spatial degrees-of-freedom in multipath propagation channels," *IEEE Trans. Ant. Propag.*, in press.

[7] K. Haneda, A. Khatun, C. Gustafson, and S. Wyne, "Spatial degrees-of-freedom of 60 GHz multiple-antenna channels," *77th Veh. Tech. Conf.*, Dresden, Germany, May 2013, accepted.

[8] M. L. Morris, M. A. Jensen, and J. W. Wallace, "Superdirectivity in MIMO systems," *IEEE Trans. Ant. Prop.*, vol. 53, no. 9, pp. 2850–2857, Sep. 2005.

[9] M. Steinbauer, A. F. Molisch, and E. Bonek, "The double-directional radio channel," *IEEE Ant. Prop. Mag.*, vol. 43, no. 4, pp. 51–63, Aug. 2001.

[10] A. A. Glazunov, M. Gustafsson, A. F. Molisch, F. Tufvesson, and G. Kristensson, "Spherical vector wave expansion of Gaussian electromagnetic fields for antenna-channel interaction analysis," *IEEE Trans. Ant. Prop.*, vol. 57, no. 7, pp. 2055–2067, July 2009.

[11] J. E. Hansen, *Spherical near-field antenna measurement,* IEE Electromagnetic waves series 26, Peter Peregrinus, London, UK, 1998.

[12] A. A. Glazunov, M. Gustafsson, A. F. Molisch, and F. Tufvesson, "Physical modeling of MIMO antennas and channel by means of the spherical vector wave expansion," *IET Microwaves, Antennas and Propagation*, vol. 3, no. 2, pp. 214–227, Mar. 2009.

[13] V.-M. Kolmonen, P. Almers, J. Salmi, J. Koivunen, K. Haneda, A. Richter, F. Tufvesson, A. F. Molisch, and P. Vainikainen, "A dynamic dual-link wideband MIMO measurement system for 5.3 GHz," *IEEE Trans. Inst. Meas.*, vol. 59, no. 4, pp. 873–883, April 2010.

[14] J. Salmi, A. Richter, and V. Koivunen, "Detection and tracking of MIMO propagation path parameters using state-space approach," *IEEE Trans. Sig. Proc.*, vol. 57, no. 4, pp. 1538–1550, April 2009.

[15] J. Poutanen, J. Salmi, K. Haneda, V.-M. Kolmonen, and P. Vainikainen, "Angular and shadowing characteristics of dense multipath components in indoor radio channels," *IEEE Trans. Ant. Prop.*, vol. 59, no. 1, pp. 245–253, January 2011.

[16] S. Takahashi and Y. Yamada, "Propagation-loss prediction using ray tracing with a random-phase technique, *IEICE Trans. Fundamentals*, vol. E81-A, no. 7, pp. 1445–1451, July 1998.